DALTON
FULL PAPER

New sandwich complexes of praseodymium(III) containing triazacyclohexane ligands†

Randolf D. Köhn,* Zhida Pan, Gabriele Kociok-Köhn and Mary F. Mahon

Department of Chemistry, University of Bath, Bath, UK BA2 7AY

Received 23rd November 2001, Accepted 21st March 2002
First published as an Advance Article on the web 3rd May 2002

N-substituted 1,3,5-triazacyclohexanes (R_3TAC) react with praseodymium trifluoromethane sulfonates [Pr(OTf)$_3$] to give the corresponding complexes, containing one or two R_3TAC ring(s) coordinated to praseodymium, depending on R. The crystal and molecular structures of these compounds have been determined by X-ray diffraction. The complex containing two coordinated R_3TAC is mononuclear, while the complex containing one R_3TAC is dinuclear with three triflate bridges. NMR diffusion studies indicate that these structures also occur in benzene solution.

1 Introduction

Many complexes containing triazacyclononane and larger macrocyclic amines are known.[1,2] They are used, for example, as bioinorganic model systems, reagents with high metal ion selectivity or as olefin polymerization catalysts. N-substituted 1,3,5-triazacyclohexane (R_3TAC) is arousing more and more interest in coordination chemistry.[3] It is easily prepared by reaction of formaldehyde with primary amines, allowing for a large variety of alkyl substituents. A wide range of complexes with transition metals (like titanium complex **A**[4] in Fig. 1) and main group elements are well established. MAO-activated chromium(III) complexes[5] (*e.g.* **B** in Fig. 1) are highly active homogeneous ethylene polymerization catalysts that resemble the Phillips catalyst in many important properties.[3,5] We are interested in expanding this chemistry into the lanthanides. Their organometallic coordination chemistry is dominated by cyclopentadienyl complexes,[6] which often give highly active catalysts for the polymerization of olefins (especially polar monomers such as MMA[7]) but they are also highly air and moisture sensitive, which limits their industrial applicability. As many features of metal complexes containing R_3TAC, such as the ring centroid–metal distance, donor orbital orientation or positions of the ring substituents resemble those of analogous Cp rather than triazacyclononane complexes, we expected that R_3TAC complexes of the lanthanides should have similar structures. Many lanthanide complexes containing macrocyclic ligands with N and O donor atoms are known and the solution chemistry in mostly polar solvents or even water is well established.[8] However, there are only a few reports on complexes with ligands containing only tertiary amine donor groups in non-polar and weakly coordinating solvents which would be compatible with aluminium alkyl co-catalysts in organometallic catalysis. A few *N*-alkyl-substituted triazacyclononane complexes of scandium and yttrium,[9] such as **C** shown in Fig. 1, exist in the literature to date, with no R_3TAC complexes being documented.

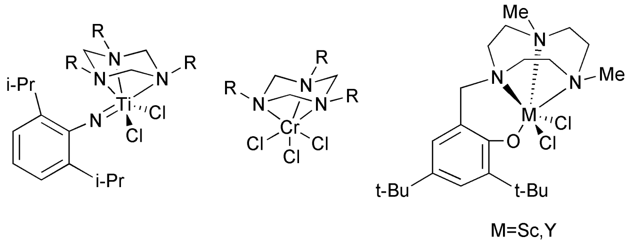

A **B** **C**

Fig. 1 Structures of some known complexes with R_3TAC and triazacyclononane.

In this paper we describe the synthesis of 1,3,5-triazacyclohexane complexes of praseodymium, as potentially useful precursors for organometallic chemistry and catalysis.

2 Results and discussion

Treatment of praseodymium trifluoromethane sulfonate, Pr(OTf)$_3$, with 1,3,5-trimethyl-1,3,5-triazacyclohexane in toluene afforded [(η^3-Me$_3$TAC)$_2$Pr(OTf)$_3$] in 65% yield. Pale green crystals were obtained by cooling the concentrated toluene solution to 4 °C. The sandwich-type complex was formed even when a 1 : 1 ratio of starting materials was used.

Among the four possible chair conformers, the all-equatorial arrangement of the methyl groups in the free ligand Me$_3$TAC occurs only in small amounts. After the formation of the η^3-compound illustrated in Fig. 2, all three methyl groups occupy equatorial sites, with very large Pr–N–R angles varying from 126 to 137°, thereby dramatically reducing the steric effects of the N-substituents (Scheme 1).

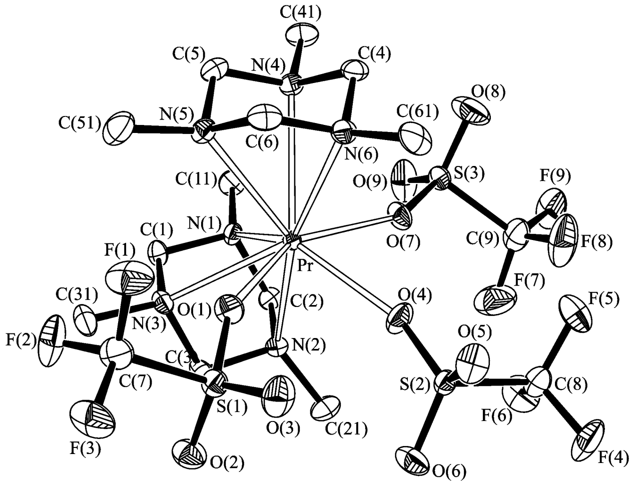

Fig. 2 Molecular structure of [(η^3-Me$_3$TAC)$_2$Pr(OTf)$_3$], with thermal ellipsoids drawn at the 50% probability level.

---

† The chemistry of 1,3,5-triazacyclohexane complexes. Part 10.[23]

Electronic supplementary information (ESI) available: UV-Vis spectrum of [(Me$_3$TAC)$_2$Pr(OTf)$_3$] in THF, plot of additional diffusion data for the peaks at 30 and 34 ppm in the ^{1}H NMR spectrum of [(Me$_3$TAC)$_2$Pr(OTf)$_3$] and rotatable 3-D crystal structure diagrams in CHIME format. See http://www.rsc.org/suppdata/dt/b1/b110784b/

DOI: 10.1039/b110784b

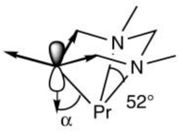

Scheme 1

Due to the rigid nature of the triazacyclohexane ring, the nitrogen lone pairs cannot be directed to the metal centre. Since there is no apparent unusual distortion in the ligand, the nitrogen lone pairs can be estimated to form angle, *α*, of 21–28° with the Pr–N axis, compared to 23–26° in analogous chromium complexes. The average N–Pr–N angle is as acute as 52°. As one might expect, due to shorter metal–nitrogen distance, transition metal complexes usually have a larger N–metal–N angles. For example, the average N–Ti–N in $[Ti(NBu^t)(Me_3TAC)Cl_2]$ is 59°,[10a] 60–63° for chromium in $[(^iPr_3TAC)CrCl(CH_2SiMe_3)_2]$,[10b] 61° for iron in $[(Me_3TAC)FeCl_3]$[10b] and 62° for copper in $[(Me_3TAC)_2CuCl_2]$.[10c] Calcium(II) has a comparable ionic radius to lanthanide(III) ions, leading to a 53° N–Ca–N angle in $[(Me_3TAC)_2Ca[P(SiMe_3)_2]_2]$.[10d] The acute angle in $[(\eta^3\text{-}Me_3TAC)_2Pr(OTf)_3]$ ultimately leads to severely misdirected nitrogen lone pairs, concomitant with a weakened N–Pr interaction. As the dipole orientation of the amine donor coincides with the direction of the lone pair, this weakening should occur even when the N–Ln interaction is purely charge–dipole (~cos *α*). Indeed, the complex is highly air and moisture sensitive and becomes sticky immediately on exposure to air.

The average Pr–N bond length of 2.663 Å for $[(\eta^3\text{-}Me_3TAC)_2Pr(OTf)_3]$ is very close to the average Pr–C(Cp) distance in $[(C_5Me_5)_2Pr(\mu\text{-}Cl)_2Na(dme)_2]$[10] (2.770 Å). The coordination number of the metal in $[(\mu^3\text{-}Me_3TAC)_2Pr(OTf)_3]$ is nine. Praseodymium has the second largest ionic radius in the lanthanide series ($r_{Pr^{III}}$ = 1.18 Å),[11] and it prefers high coordination numbers, as exhibited in $[(C_5H_5)_3Pr]_\infty$ and $[(C_5H_5)_3PrCNC_6H_{11}]$ (both coordination number ten), unless stabilized by very bulky ligands, as in the case of $[\{C_5H_3(SiMe_3)_2\}_2PrCl]_2$, where the Pr is 8-coordinate.[12]

The UV-Vis spectrum of $[(\eta^3\text{-}Me_3TAC)_2Pr(OTf)_3]$ in THF shows the typical narrow absorption bands at half intensity of about 50 cm^{-1} and is almost identical to that of $Pr(OTf)_3$ in water, showing little influence from the ligand environment.

On carrying out the same reaction in THF, the product yield increased from 65 to 81%. Crystals obtained from this reaction had the same unit cell data as those obtained from the toluene reaction.

The ligand signals in ^{1}H-NMR spectra of the complex are shifted and broadened relative to free Me_3TAC due to the paramagnetism of the complex. The ^{1}H-NMR spectrum in d_6-benzene shows two signals of about 80 Hz wide at $\delta = 46$ and 30 in a ratio of 1 : 1. We assigned these to the pair of *exo*- and *endo*-hydrogen atoms of the ring. A less broad signal ($\Delta\nu_{1/2}$ = 20 Hz) at $\delta = 8.6$ can be assigned to the methyl groups shifted by praseodymium. All spectra also contained signals for uncoordinated Me_3TAC at 3.5 and 2.0 ppm and an additional set of broader signals at 41, 34 and 14.0 ppm in a 1 : 1 : 3 ratio, which we assigned to another Me_3TAC–Pr complex occurring in solution. Upon dilution with further benzene, it was noticed that the relative intensity for the free ligand and the entire set of broad peaks increased slightly, while the signal at 8.6 ppm decreased. This equilibrium can be described by Scheme 2, with

$$2\,[L_2Pr(OTf)_3] \xrightleftharpoons{K} [LPr(OTf)_3]_2 + 2\,L$$

$$L = Me_3TAC$$

Scheme 2

a *K* of about 8 × 10^{-5} mol L^{-1} at room temperature. We performed a PGSE[13] diffusion study on the solution to establish the size of the two praseodymium complexes found in solution (Fig. 3). The diffusion constant for the complex giving rise to the signal at 8.6 ppm (6.9 × 10^{-10} $m^2\,s^{-1}$) agrees well with the value expected for $[(Me_3TAC)_2Pr(OTf)_3]$ and the major set of signals can be assigned to the complex found in the crystal structure. The diffusion constant for the minor complex causing the signal at 14 ppm (5.1 × 10^{-10} $m^2\,s^{-1}$) is close to the value expected for the dinuclear complex shown in Scheme 2. The simultaneously determined diffusion constants for free Me_3TAC (9.3 × 10^{-10} $m^2\,s^{-1}$) and benzene (19 × 10^{-10} $m^2\,s^{-1}$) also agree with the expected values.[14]

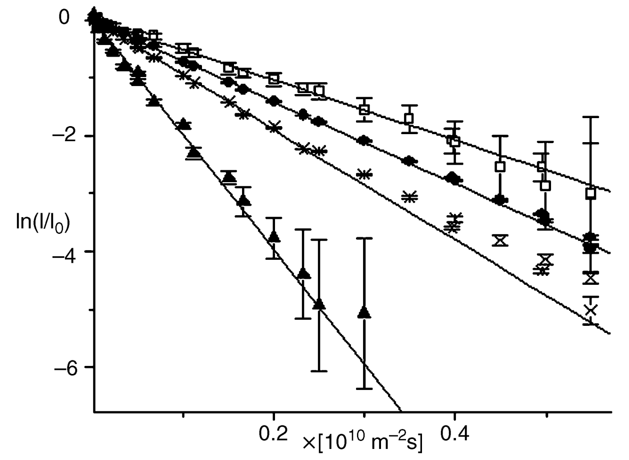

Fig. 3 ^{1}H diffusion data for a solution of $[(Me_3TAC)_2Pr(OTf)_3]$ (●) in C_6D_6 (▲). The data for the product (□) of the dissociation of Me_3TAC (×) corresponds to the diffusion constant expected for a dinuclear complex.[14]

In an attempt to isolate this dimeric complex, the reactions were repeated with the slightly bulkier Et_3TAC and $Pr(OTf)_3$ (Scheme 3). Crystals grown from toluene revealed a dinuclear complex containing an additional $[EtNH_3]^+[OTf]^-$ (molecular structure shown in Fig. 4). The $[EtNH_3]^+[OTf]^-$ probably comes from a small amount of ethylamine in Et_3TAC and excess HOTf in $Pr(OTf)_3$. The bond lengths and angles are nearly identical to those in $[(\eta^3\text{-}Me_3TAC)_2Pr(OTf)_3]$. However, the two praseodymium atoms of the dinuclear complex have a different coordination environment. The coordination number of Pr(1) is nine, with three Pr–N bonds to Et_3TAC (average bond length 2.66 Å), three Pr–O bonds to three bridging triflates (2.46 Å), one Pr–O bond to a terminal η^1-triflate (2.39 Å) and two Pr–O bonds to an η^2-triflate (2.58 Å). The coordination number of Pr(2) is eight, with a coordination environment similar to Pr(1), except for the presence of two terminal η^1-triflates (2.37 Å) instead of one η^1- and one η^2-triflate. The three Pr–N bonds (2.65 Å) and the three Pr–O bonds to the bridging triflates (2.43 Å) are also slightly shorter than for Pr(1), as expected for the lower coordination number. All three terminal η^1-triflates are also hydrogen bridged to the $[EtNH_3]^+$ cation (N ··· O 2.8–3.0 Å), whereas the terminal η^2-triflate is not, which may explain the observed asymmetry.

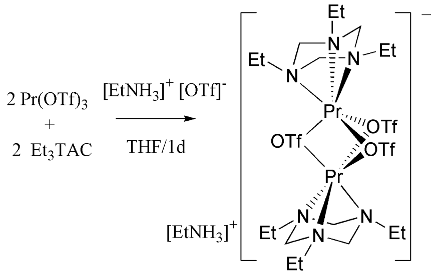

Scheme 3

We repeated the reaction, adding the stoichiometric amount of $[EtNH_3]^+[OTf]^-$, and the elemental analysis of the product agreed with the structure of the dimer.

Table 1 Crystal data and structure refinement for $(Me_3TAC)_2Pr(OTf)_3]$ and $[EtNH_3][(Et_3TAC)_2Pr_2(OTf)_7]\cdot(C_7H_8)_{0.5}$

Compound	$(Me_3TAC)_2Pr(OTf)_3$	$[EtNH_3][(Et_3TAC)_2Pr_2(OTf)_7]\cdot(C_7H_8)_{0.5}$
Empirical formula	$C_{15}H_{30}F_9N_6O_9PrS_3$	$C_{30.5}H_{54}F_{21}N_7O_{21}Pr_2S_7$
M/g mol^{-1}	846.54	1760.05
Crystal colour	Pale green	Yellow
Crystal size/mm	0.25 × 0.2 × 0.1	0.35 × 0.3 × 0.2
Crystal system	Orthorhombic	Monoclinic
Space group	$Pna2_1$ (no. 33)	$P2_1/n$ (no. 14)
a/Å	14.7680(2)	10.4270(1)
b/Å	13.3330(2)	54.2090(4)
c/Å	15.1600(2)	11.1980(1)
β/°		97.7190(4)
U/Å^3	2985.03(7)	6272.17(9)
Z	4	4
D_c/g cm^{-3}	1.884	1.864
μ(Mo-Kα)/mm^{-1}	1.951	1.901
F(000)	1688	3492
$2\Theta_{range}$/°	6–55	6–50
Collected data	28951	24339
Unique data ($I > 2\sigma I$) [R(int)]	6651 [0.041]	9182 [0.0497]
Refined parameters	388	766
Min./max e$^-$ density/e Å^{-3}	−0.609/0.395	−1.044/1.224
Absolute structure param., χ[a]	−0.020(6)	
R_1[b] ($I > 2\sigma I$)	0.0214	0.0577
wR_2[c] ($I > 2\sigma I$)	0.0453	0.1283
GOF[d]	1.054	1.050

[a] H. D. Flack, *Acta Crystallogr., Sect. A*, 1983, **39**, 876. [b] $R_1 = \Sigma\,||F_o| - |F_c||/\Sigma|F_o|$. [c] $wR_2 = \{\Sigma[w(F_o^2 - F_c^2)^2]/\Sigma[w(F_o^2)^2]\}^{1/2}$. [d] $GOF = S = \{\Sigma[w(F_o^2 - F_c^2)^2]/(n - p)\}^{1/2}$.

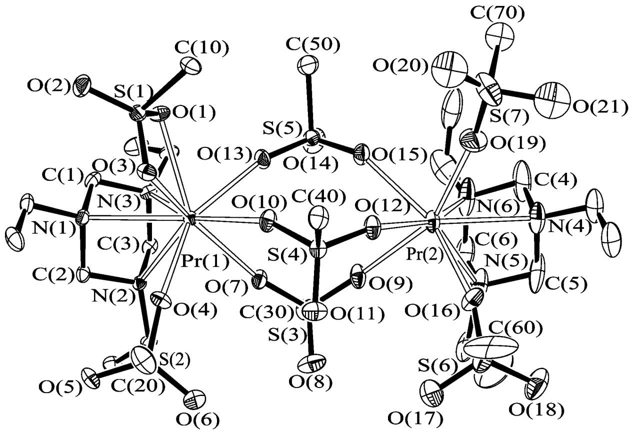

Fig. 4 Structure of $[(Et_3TAC)_2Pr_2(OTf)_7]^-$ with thermal ellipsoids drawn at the 20% probability level.

From the corresponding NMR spectra, we found signals due to the *endo*- and *exo*- hydrogen atoms of the ring at lower fields than for $[(\eta^3\text{-}Me_3TAC)_2Pr(OTf)_3]$, 56 and 47 ppm, respectively. The signal due to CH_2 in the *N*-ethyl group is at about 18 ppm, which is close to the value of 14 ppm found for the $N\text{–}CH_3$ signal of the minor component proposed in Scheme 1. This is also evidence for a similar dimeric structure for this minor component.

The above study demonstrates that mono- and bis-R_3TAC complexes of the lanthanides can be prepared, and we are currently studying their catalytic capabilities.

3 Experimental

All manipulations of air- and moisture-sensitive compounds were carried out under an atmosphere of nitrogen or argon using standard Schlenk-line or glove box techniques. Solvents were dried according to standard methods and collected by distillation. Praseodymium triflate was prepared according to literature method.[15] Me_3TAC and Et_3TAC were prepared according to the literature[16] and were dried by distillation from sodium. ^1H and ^{13}C NMR spectra were recorded on Varian Mercury-400 or Bruker Avance-300 instruments. A modified version (BPPSTE)[17] of the pulsed field gradient spin echo (PGSE) sequence was used to determine the diffusion constants.[13] The samples were measured at 400 MHz at 293 K without spinning. The gradient pulse was varied up to a gradient strength (G) of about 0.2 T m^{-1} with a constant duration (δ) of 10 ms followed by a delay (τ) of 0.3 ms. The time between the midpoints of the gradients (Δ) was chosen as 30 ms. The diffusion constant (D) was obtained as the slope of a plot of $\ln(I/I_0) = -Dx$, with I being the observed intensity, I_0 the intensity without gradient and $x = (\gamma_H\delta G)^2(\Delta - \delta/3 - \tau/2)$.[17] The gradient strength was calibrated using the diffusion constant for HDO in D_2O as a reference.[18] Elemental analyses was conducted on an Exeter Analytical Instruments CE-440 elemental analyser.

3.1 Synthesis of $[(\eta^3\text{-}Me_3TAC)_2Pr(OTf)_3]$

3.1.1 Toluene as solvent. Me_3TAC (0.1 g, 0.8 mmol) and praseodymium triflate (0.47 g, 0.8 mmol) were transferred into 100 ml of toluene. The suspension was stirred at room temperature for 2 days and then decanted from the solid, which was extracted with further toluene. After concentrating to about 5 ml under reduced pressure, the clear solution was cooled to 4 °C. Pale green crystals were obtained (0.37 g, 65% yield). ^1H NMR (C_6D_6, 400 MHz): δ 46 (s, 6H, $NCH_{endo}H_{exo}N$, $\Delta\nu_{1/2}$ = 80 Hz), 30 (s, 6H, $NCH_{endo}H_{exo}N$, $\Delta\nu_{1/2}$ = 80 Hz), 8.6 (s, 18H, NMe, $\Delta\nu_{1/2}$ = 20 Hz). ^{19}F NMR (C_6D_6, 376 MHz): δ −94.8 (OTf, $\Delta\nu_{1/2}$ = 410 Hz). Anal. calcd for $C_{15}H_{30}F_9N_6O_9PrS_3$: C, 21.3; H, 3.57; N, 9.93; found: C, 21.1; H, 3.71; N, 9.53%.

3.1.2 THF as solvent. $Pr(OTf)_3$ (0.82 g, 1.4 mmol) was stirred in 50 ml THF, and Me_3TAC (0.36 g, 2.8 mmol) was added dropwise *via* syringe. After 2 h, the solution became clear and was stirred overnight. After removal of the solvent *in vacuo*, the residue was treated with 100 ml of toluene at 60 °C for 5 h and decanted while hot. Pale green crystals (0.95g, 81% yield) were obtained by cooling the solution to 4 °C, and gave identical NMR spectra and unit cell parameter to those obtained following the procedure in section 3.1.1.

3.2 Synthesis of $[EtNH_3][(Et_3TAC)_2Pr_2(OTf)_7]\cdot(C_7H_8)_{0.5}$

$Pr(OTf)_3$ (0.644 g, 1.1 mmol), Et_3TAC (0.187 g, 1.1 mmol) and $EtNH_3(OTf)$ (0.214 g, 1.1 mmol) were added to 100 ml THF.

Table 2 Selected bond lengths [Å] and angles [°] in [(Me$_3$TAC)$_2$-Pr(OTf)$_3$] (standard deviations in parentheses)

Pr–O(4)	2.399(2)	Pr–N(6)	2.600(2)
Pr–N(2)	2.612(2)	Pr–N(5)	2.690(2)
Pr–N(3)	2.693(2)	Pr–N(1)	2.712(2)
Pr–N(4)	2.730(2)	C(1)–N(3)	1.464(3)
C(1)–N(1)	1.475(3)	N(1)–C(11)	1.482(3)
S(1)–O(3)	1.431(2)	S(1)–O(1)	1.466(2)
S(1)–C(7)	1.823(3)	C(7)–F(2)	1.312(4)
O(4)–Pr–O(7)	72.99(7)	N(2)–Pr–N(1)	52.17(6)
N(3)–Pr–N(1)	51.34(6)	N(2)–Pr–N(3)	52.53(6)
O(4)–Pr–N(2)	85.27(6)	O(1)–Pr–N(2)	97.64(6)
C(1)–N(1)–C(2)	108.5(2)	C(1)–N(1)–C(11)	110.5(2)
C(21)–N(2)–Pr	127.36(15)	N(6)–Pr–N(2)	167.06(7)
S(1)–O(1)–Pr	153.96(12)	O(3)–S(1)–C(7)	102.04(13)
F(1)–C(7)–F(3)	107.3(2)	F(8)–C(9)–S(3)	112.9(2)

[a] U(eq) is defined as one third of the trace of the orthogonalized U_{ij} tensor.

Table 3 Selected bond lengths [Å] and angles [°] in [EtNH$_3$]-[(Et$_3$TAC)$_2$Pr$_2$(OTf)$_7$]·(C$_7$H$_8$)$_{0.5}$ (standard deviations in parentheses)

Pr(1)–N(1)	2.674(6)	Pr(1)–N(3)	2.640(6)
Pr(1)–N(2)	2.665(6)	Pr(1)–O(7)	2.502(6)
Pr(2)–O(9)	2.445(6)	Pr(1)–O(1)	2.579(5)
Pr(2)–O(16)	2.350(7)	Pr(2)–O(19)	2.383(8)
C(1)–N(1)	1.480(10)	C(1)–N(3)	1.474(10)
O(2)–S(1)–C(7)	104.35(12)	O(1)–S(1)–C(7)	102.43(13)
N(3)–Pr(1)–N(2)	52.07(18)	N(6)–Pr(2)–N(4)	52.5(3)
C(11)–N(1)–Pr(1)	134.0(5)	C(21)–N(2)–Pr(1)	129.3(4)

The mixture was stirred vigorously at room temperature. After one day, the THF was removed *in vacuo*, and the residue was extracted with 150 ml of hot toluene and decanted from the solid. The solution was concentrated and cooled to 4 °C to give 0.23 g of yellow crystals. The mother solution yielded a further 0.33 g of product after removal of the toluene (52% total yield). ^{1}H NMR (C$_6$D$_6$, 400 MHz): δ 56 (s, 6H, NCH$_{endo}$H$_{exo}$N, $\Delta\nu_{1/2}$ = 70 Hz), 47 (s, 6H, NCH$_{endo}$H$_{exo}$N, $\Delta\nu_{1/2}$ = 140 Hz), 18 (s, 12H, NC*H*$_2$Me), $\Delta\nu_{1/2}$ = 50 Hz), 7.0 (m, 2.5H, *Ph*Me), 4.3 (s, 18H, Me, $\Delta\nu_{1/2}$ = 30 Hz), 3.4 (br, 2H, MeC*H*$_2$NH$_3^+$), 2.4 (s, 1.5H, Ph*Me*), 1.1 (t, 3H, *Me*CH$_2$NH$_3^+$); ^{19}F NMR (C$_6$D$_6$, 376 MHz): δ −115.1 (OTf, $\Delta\nu_{1/2}$ = 350 Hz). Anal. calcd for C$_{30.5}$H$_{54}$F$_{21}$-N$_7$O$_{21}$Pr$_2$S$_7$: C, 20.8; H, 3.09; N, 5.57; found: C, 19.8; H, 3.37; N, 5.54%.

4 Crystallography

Intensity data for both structures reported here were collected at 150 K on a Nonius Kappa CCD equipped with a low temperature device, using graphite monochromated Mo-Kα radiation (λ = 0.71070 Å), and processed using the Nonius Software.[19] For structure solution and refinement, the programs SIR-97[20] and SHELXL-97/2,[21] and for the illustrations Ortep3,[22] were employed. Crystal parameters and details of the data collection, solution and refinement are summarized in Table 1. ORTEP graphics of the complexes are presented in Fig. 2 and 4, and selected bond lengths and angles in Tables 2 and 3.

Notes on the refinement: [EtNH$_3$][(Et$_3$TAC)$_2$Pr$_2$(OTf)$_7$] crystallizes with a half molecule of toluene in the asymmetric unit, which was refined isotropically. No attempt was made to calculate the missing H atoms of this solvent molecule. One of the seven triflates showed disorder in a 1 : 1 ratio and was isotropically refined using a split atom model.

CCDC reference numbers 175383 and 175384.

See http://www.rsc.org./suppdata/dt/b1/b110784b/ for crystallographic data in CIF or other electronic format.

Acknowledgements

This work has been financially supported by a Chevening fellowship of the Royal Society of the United Kingdom.

References and notes

1 P. Chaudhuri and K. Wieghard, *Prog. Inorg. Chem.*, 1987, **35**, 329–436.

2 S. Y. Bylikin, D. A. Robson, N. A. H. Male, L. H. Ress, P. Mountford and M. Schröder, *J. Chem. Soc., Dalton Trans.*, 2001, 170–180.

3 R. D. Köhn, G. Kociok-Köhn and M. Haufe, *J. Organomet. Chem.*, 1995, **501**, 303–307.

4 P. J. Wilson, A. J. Blake, P. Mountford and M. Schröder, *J. Organomet. Chem.*, 2000, **600**, 71–83.

5 R. D. Köhn, M. Haufe, S. Mihan and D. Lilge, *Chem. Commun.*, 2000, 1927–1928.

6 F. T. Edelmann and V. Lorenz, *Coord. Chem. Rev.*, 2000, **209**, 99–160.

7 H. Yasuda, E. Ihara, T. Hayakawa and T. Kakehi, *J. Macromol. Sci., Pure Appl. Chem.*, 1997, **34**, 1929–1944.

8 See, for example: V. Alexander, *Chem. Rev.*, 1995, **95**, 273–342.

9 S. Hajela, W. P. Schaefer and J. E. Bercaw, *J. Organomet. Chem.*, 1997, **532**, 45–53.

10 (*a*) P. J. Wilson, P. A. Cooke, A. J. Blake, P. Mountford and M. Schröder, *New J. Chem.*, 1999, 271–273; (*b*) R. D. Köhn and G. Kociok-Köhn, *Angew. Chem., Int. Ed. Engl.*, 1994, **33**, 1877–1878; (*c*) R. D. Köhn, G. Seifert and G. Kociok-Köhn, *Chem. Ber.*, 1996, **129**, 1327–1333; (*d*) M. Westerhausen and W. Schwarz, *J. Organomet. Chem.*, 1993, **463**, 51–63.

11 R. D. Shannon, *Acta Crystallogr., Sect. A*, 1976, **32**, 751.

12 H. Schumann, I. Albrecht, J. Loebel and E. Hahn, *Organometallics*, 1986, **5**, 1296–1304, and references therein.

13 For recent applications in coordination chemistry see, for example: D. Drago, P. S. Pregosin and A. Pfaltz, *Chem. Commun.*, 2002, 286–287; M. Valentini, P. S. Pregosin and H. Rüegger, *Organometallics*, 2000, **19**, 2551–2555.

14 The diffusion constant can be estimated for approximately spherical particles using the Stokes–Einstein equation: $D = k\mathrm{T}/(n\pi\eta r)$, where k = Boltzmann constant, T = absolute temperature, η = viscosity of the solvent, r = radius of the sphere, and n = 6 for large spheres and n = 4 for r < 5 Å (see, for example: S. Beck, A. Geyer and H.-H. Brintzinger, *Chem. Commun.*, 1999, 2477–2478). The investigated molecules had radii near 5 Å and the expected range of radii (and volumes) with n = 4–6 for D = 9.3, 6.9 and 5.1 (all 10^{-10} m^2 s^{-1}) are 3.3–5.0 (150–520), 4.4–6.7 (360–1260) and 6.1–9.1 Å (950–3160 Å^3), respectively. Ignoring empty volumes, the molar volumes of Me$_3$TAC (233 Å^3) and [(Me$_3$TAC)$_2$Pr(OTf)$_3$] (746 Å^3) can be estimated from their respective densities and are well within the range estimated from D. The molar volume of the dinuclear complex [EtNH$_3$][(Et$_3$TAC)$_2$Pr$_2$(OTf)$_7$]·(C$_7$H$_8$)$_{0.5}$ (X-ray: 1568 Å^3) can be used to estimate the volume of the dinuclear complex [(Me$_3$TAC)$_2$Pr$_2$(OTf)$_6$] by subtracting the difference in volume between Et$_3$TAC and Me$_3$TAC (2 × 85 Å^3) and the volumes of EtNH$_2$ (110 Å^3), HOTf (147 Å^3) and toluene (0.5 × 177 Å^3), giving1050 Å^3, which is very close to the volume found for n = 6.

15 M. El, M. Hamidi and J. Pascal, *Polyhedron*, 1994, **13**, 1787–1792.

16 R. D. Köhn, M. Haufe, G. Kociok-Köhn and A. C. Filippou, *Inorg. Chem.*, 1997, **36**, 6064–6069.

17 M. D. Pelta, H. Barjat, G. A. Morris, A. L. Davis and S. J. Hammond, *Magn. Reson. Chem.*, 1998, **36**, 706–714.

18 H. J. W. Tyrell and K. R. Harris, *Diffusion in Liquids*, Butterworths, London, 1984.

19 Z. Otwinowski and W. Minor, *DENZO-SMN Manual*, University of Texas Southwestern Medical Center, Dallas, 1996.

20 A. Altomare, M. C. Burla, M. Camalli, G. L. Cascarano, C. Giacovazzo, A. Guagliardi, A. G. G. Moliterni, G. Polidori and R. Spagna, *J. Appl. Crystallogr.*, 1999, **32**, 115–119.

21 G. M. Sheldrick, SHELXL97-2, Program for Crystal Structure Refinement, Universität Göttingen, Germany, 1998.

22 L. J. Farrugia, J. Appl. Crystallogr., 1997, **30**, 565.

23 Part 9: R. D. Köhn, M. Haufe, G. Kociok-Köhn, S. Grimm, P. Wasserscheid and W. Keim, *Angew. Chem.*, 2000, **112**, 4519–4521; R. D. Köhn, M. Haufe, G. Kociok-Köhn, S. Grimm, P. Wasserscheid and W. Keim, *Angew. Chem., Int. Ed.*, 2000, **39**, 4337–4339.